Lateral Bending of Ag Nanowires Towards Controllable Manipulation

Licong Cui[1], Jiaming Li[2], Huaicheng Zhou[1], Lei Wu[1], Dan Yang[1], Huiyun Liu*[,3], Linmao Qian*[,1], Bingjun Yu*[,1]

[1] *Tribology Research Institute, School of Mechanical Engineering, Southwest Jiaotong University, Chengdu 610031, China*

[2] *ZTE Corporation, Chengdu 610299, China*

[3] *Department of Electronic & Electrical Engineering, University College London, London WC1E 7JE, U.K.*

* Corresponding authors:

huiyun.liu@ucl.ac.uk (HYL); linmao@swjtu.edu.cn (LMQ); bingjun@swjtu.edu.cn (BJY)

ABSTRACT

Nanowires (NWs) provide opportunities for building high-performance sensors and devices at micro/nanoscales. Directional movement and assembly of NWs have attracted extensive attention; however, controllable manipulation remains challenging partly due to the lack of understanding on interfacial interactions between NWs and substrates (or contacting probes). In the present study, lateral bending of Ag NWs was investigated under various bending angles and pushing velocities, and the mechanical performance corresponding to microstructures was clarified based on high-resolution transmission electron microscope (HRTRM) detections. The bending angle-dependent fractures of Ag NWs were detected by an atomic force microscope (AFM) and a scanning electron microscope (SEM), and the fractures occurred when the bending angle was larger than 80°. Compared with Ag substrate, Ag NWs exhibited a lower system stiffness according to the nanoindentation with an AFM probe. HRTRM observations indicated that there were grain boundaries inside Ag NWs, which would be the contributor to the fractures and cracks generation on Ag NWs during lateral bending and nanoindentation. This study provides a guide to controllably manipulate NWs and fabricate high-performance micro/nanodevices.

KEYWORDS: *Nanowires, Nanomanipulation, Lateral bending, Mechanical performance, AFM*

INTRODUCTION

Nanomaterials have been extensively applied in the field of catalysis, sensor, and energy because of their unique chemical and physical properties, such as superb electrical conductivity, excellent heat conductivity, chemical stability, advanced optical properties, and high mechanical strength.[1-4] As one-dimensional nanomaterials, nanowires (NWs) have indispensable roles in biomedicine, photonics, electronics, and energy applications.[5,6] It is highly noted that the manipulation of NWs offers the possibility to assemble high-performance devices, for instance, energy storage devices, highly sensitive sensors, electrochromic devices, nanowire switches, and photodetectors.[7-12] However, due to the manipulation of NWs involves a complicated process with interfacial interactions (*e.g.*, nanoscale adhesion and friction) and deformations, realizing high-precision manipulation remains a huge challenge.[13]

As a powerful nanotechnology tool, scanning probe microscope (SPM), including atomic force microscopy (AFM), can be used not only for nanoscale imaging but for manipulating nanoscale objects such as NWs.[14-16] Nevertheless, SPM can hardly enable both imaging and manipulation simultaneously; therefore, the manipulation process is generally invisible. Currently, the integration of SPM and visualization equipment enables the possibility for precise manipulation of NWs. With the visualization by scanning electron microscope (SEM), transmission electron microscope (TEM), or high-resolution optical microscope (OM), NWs can be driven by vibration, mechanical pushing, picking and placing with flexible probes.[17-19] During the manipulation, visual NWs on substrates are transferred to the manipulation unit, and subsequently NWs can

be moved in real time under the feedback process with better convenience and manipulation accuracy. As the modified SPM-based manipulation tools, nanotweezers consisting of two microcantilevers can grab and drop individual NW through vibrating at a certain frequency, achieving the picking and placing of NWs.[20,21] By controlling the interfacial interactions between NWs and microcantilevers, such as electrostatic force and Van der Waals force, the nanotweezers are highly potential for directional movement of NWs.[22]

Even though SPM provides much flexibility for NWs manipulation, the underlying issues, including interfacial interactions and mechanical performances at the nanoscale, remain to be fully investigated and clarified for controllable manipulation and assembly of NWs. Adhesive exists widely in nanoscale contact and can be affected by the sliding velocity of a nanoscale tip.[23,24] Such adhesion would play an important role in governing interfacial interactions between the NW and the substrate (or the tip). For instance, SPM is inefficient in manipulating individual NW due to the adhesion between the NW and the substrate (or the tip), resulting in the inability to drive NWs at times.[21] Therefore, the understanding of interfacial adhesion can effectively promote the progress on picking and placing NWs towards controllable manipulation. Meanwhile, the mechanical properties (*e.g.*, bending dynamics and the ultimate fracture strength) of NWs can be investigated with the help of the adhesion between the NW and the substrate.[25] In addition, for obtaining optimal manipulation parameters by an AFM probe, lateral bending-dependent deformation and movement of individual NW under different conditions remain to be investigated.

In this study, bending angles, pushing velocities, and contact positions were taken into account during the lateral bending of Ag NWs by an AFM probe. The mechanical performance was investigated by nanoindentation test. For interpreting the interfacial adhesion and structure-response mechanical property, the cross-section microstructure of individual Ag NW was investigated by high-resolution TEM. Relevant research can lay a foundation for the subsequent assembly of NWs-based devices.

RESULTS AND DISCUSSION

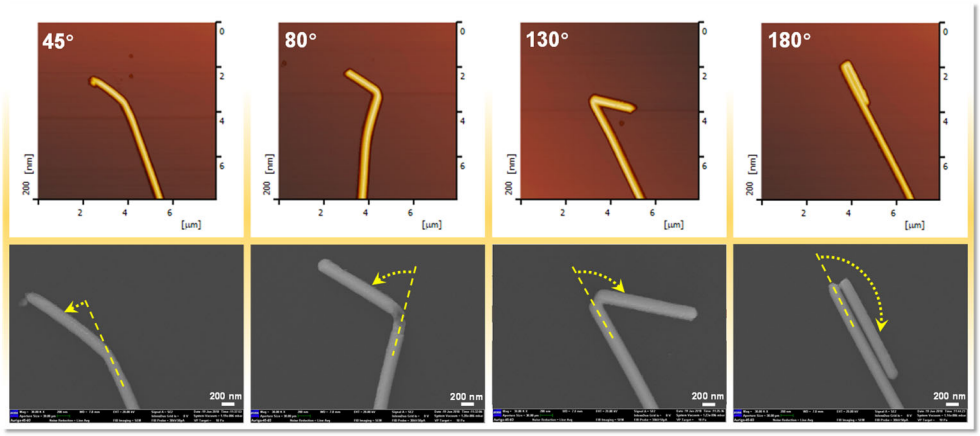

Figure 1. Ag NWs after being bent at angles θ of 45°, 80°, 130°, and 180°, respectively. AFM images of the NWs on the top were acquired under tapping mode, corresponding to SEM images at the bottom.

Bending angle-dependent deformation of Ag NWs. During the manipulation process, NWs can be bent by a lateral force,[26] and mechanical deformation or fracture may occur at the bending position. However, few attentions are paid to the fracture or the crack of NWs during bending. In this study, Ag NWs were bent by an AFM probe at different angles of 45°, 80°, 130°, and 180°, respectively, as shown in Figure 1. From AFM images in the top of Figure 1, deformed NWs can be detected after being bent,

and hardly any fracture was observed due to the tip radius limitation in the scanning. Nevertheless, obvious fractures can be found in the bending region by high-resolution SEM observation (the bottom of Figure 1). It was noted that the fracture started to happen at a bending angle of 80°. Bending at a larger angle would exacerbate the fracture, and the NW was broken at 180°.

Nanoindentation test. To further understand the fracture mechanism of NWs during lateral bending, nanoindentation tests were performed on Ag NWs as well as Ag substrate by an AFM tip. Figure 2a and b displayed a comparison of indentations under the same indentation depth. Significantly, surface cracks were detected beside the indentation on the NW, as illustrated by the arrow in Figure 2a, while material pileups were observed beside the indentation on the substrate. From the cross-section profiles in Figure 2c, the residual depth of the indentation on the substrate was larger than that on the NW. Therefore, it can be further inferred that the hardness and brittleness of Ag NWs were relatively high so that extended cracks would appear on the surface; while the ductility of Ag substrate was relatively better, and hence a greater indentation depth could be obtained. Moreover, the slope of the force curve measured from the indentation process on Ag NWs was smaller than that on Ag substrate, suggesting that Ag NWs presented a lower system stiffness.[27] Since the system stiffness of one-dimensional materials is small, the combined actions of the lateral force introduced by AFM probe driving and interfacial interactions may lead to obvious bending deformation of the manipulated object, which can be regarded as a beam structure within a certain aspect ratio range, and the Euler-Bernoulli equation can be employed to describe the

deformation behavior of such one-dimensional materials.[28,29] Accordingly, the changes in NWs' topography on the substrate before and after manipulation depend on the mechanical properties of the NW itself, interfacial interactions, and the lateral force.

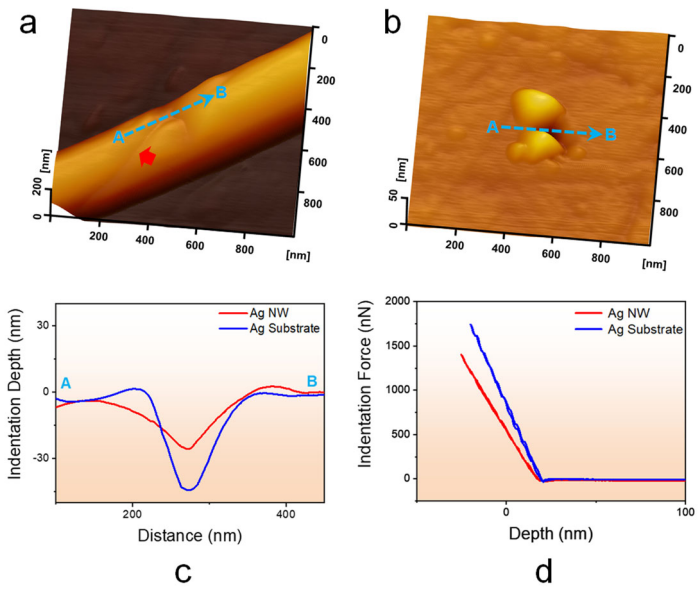

Figure 2. Comparison of nanoindentation results on Ag NWs and Ag substrates. (a) AFM image of the indentation on the NW. (b) AFM image of the indentation on the substrate. (c) Cross-section profiles of the indentations obtained from the dotted lines on (a) and (b). (d) Indentation force-depth curves measured from the indentations process.

Considering the strong interfacial interactions between the NW and the substrate, the bending of the NW may lead to its fracture. When the tip continuously pushes one end of the NW towards the other, the curvature of the bending part and the bending energy stored in the NW increases in succession. Since the interfacial interactions between the NW and the substrate are strong enough, the release of bending energy will

be hindered, that is, the other end of the NW will not spring away. The point of maximum normal stress appears outside the position of maximum curvature, and when the maximum stress exceeds the tensile limit, the NW will crack from there. The bending energy U can be calculated from Eq. (1), where S, E, I, and φ stand for NW arc length, elastic modulus, section moment, and bending angle.[18]

$$U = \int_0^S \frac{EI}{2}\left(\frac{d\varphi}{ds}\right)^2 ds \quad (1)$$

Effect of tip-driving velocity on manipulation. For lateral manipulation of NWs, tip-driving velocities can affect the precision of distance control during moving and positioning.[30] In the present study, a series of tip-driving-velocity-dependent movements of Ag NWs were investigated at tip-driving velocities of 0.1, 1.0, and 10.0 μm/s for optimizing the manipulation process. Throughout the tests, the tip-contact position on NWs, *i.e.*, the middle and end part, was also considered for NWs manipulation. For obtaining comparable results, 15 μm-long NWs were chosen for the manipulation, and the normal load applied on the AFM tip for the manipulation was set as 130 nN. Figure 3 demonstrated the results of manipulation on the end and the middle part of the NW at the velocity of 0.1 μm/s, respectively. When the NW was pushed on the end, the maximum lateral force immediately reached ~280 nN once the tip contacted the NW, and then decreased with the tip moving, as shown in Figure 3b. The sudden increase in lateral force can be partly ascribed to the static friction at the beginning of the NW sliding,[31] where the static friction was expected from the adhesion between the NW and the substrate. It was also noted that the span of lateral force mutation was consistent with the moving distance of the NW. In contrast, the lateral force measured

from the middle part of the NW was much higher than that from the end during the manipulation, as displayed in Figure 3e. In order to address NWs manipulation, we propose a simplified mechanical model (Figure 3c and f), where F_l is the lateral force applied by AFM probe driving and F_s is the combined force of the interfacial interactions between the NW and the substrate, including adhesion and friction. Since AFM probe pushes more parts of the NW to move during the manipulation on the middle part of the NW than that of the manipulation on the end, which means a larger contact area between the part of the NW driven by the AFM probe and the substrate at this moment, and a larger contact area will result in stronger interfacial adhesion,[32] that is, it takes a larger F_l to offset the effect of F_s to complete the manipulation. Additionally, a negative lateral force was detected when the tip left the NW (Figure 3b and e), which could be resulted from the interaction during the separating of the tip from the NW, such as the adhesion between the substrate and the NW.

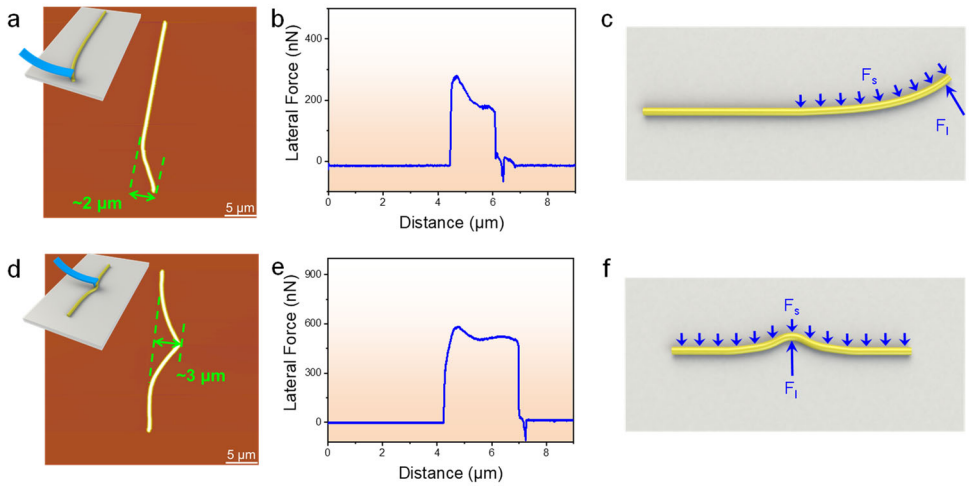

Figure 3. AFM images and lateral force for the manipulation of Ag NWs at the velocity of 0.1 μm/s. (a, d) The span of the NW manipulation positions. (b, e) Lateral force

collected during the manipulation on the end and the middle of the NW. (c, f) The simplified mechanical model for NWs manipulation. The insets on (a, d) show the schematics of the manipulation.

For comparison, the lateral manipulation was also performed at 1 and 10 μm/s, respectively. The manipulation at 1 μm/s on the end part of the NW (Figure 4a) was not significantly different from that at 0.1 μm/s in Figure 3b, and only a slight negative lateral force was detected upon tip's going away from the NW, owing to the adhesion between the tip and the NW decreased with increasing separation speed.[33] Similarly, the manipulation on the middle part of the NW can lead to higher lateral force than that from the end. However, the manipulation at 10 μm/s was significantly different from the above results, especially for the manipulation on the middle (Figure 4d). When the NW was pushed on the middle at 10 μm/s, it can be easily removed from the substrate, leaving some adhesion marks. Moreover, the lateral force gone up rapidly with the NW being pushed away as displayed in Figure 4d, and the corresponding lateral force curve was not enclosed. One possible mechanism is that the AFM probe approaches the NW at a relatively high velocity (10 μm/s), at which the momentum of the AFM probe is larger than that at 0.1 μm/s and 1 μm/s. After contacting the NW, momentum transfer occurs between the NW and the probe so that the NW is also of high momentum, which rapidly breaks the adhesion between the NW and the substrate. Since the interfacial interactions between the NW and the substrate always hinder the movement of the NW, more parts of the NW are pushed to offset the high momentum delivered by the AFM probe at 10 μm/s, and this will gradually drive the whole NW to move. As a result, the

lateral force continues to increase due to the constantly enlarging contact area between the part of the NW driven by the AFM probe and the substrate. During the manipulation, the AFM probe keeps contact with the NW at all times, thus the lateral force curve is also not enclosed. Combining Figures 3 and 4, it was also noted that the distance of the NW movement, which was consistent with the span of the force mutation, increased with the driving velocity from 0.1 to 10 μm/s.

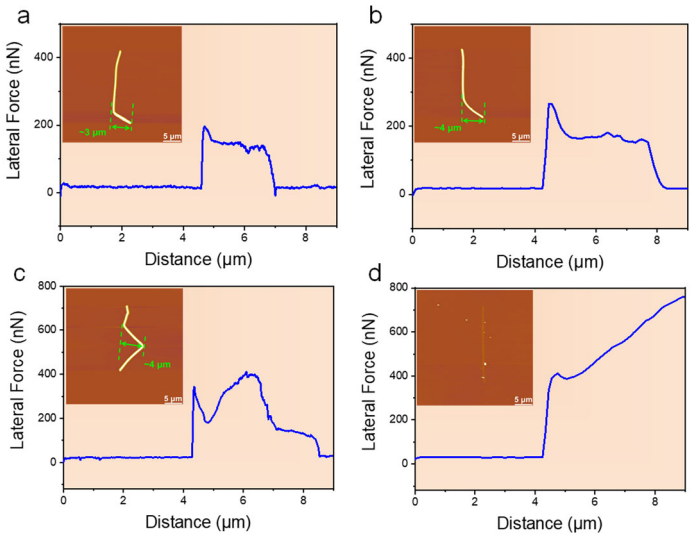

Figure 4. AFM images and lateral force for the manipulation of Ag NWs at driving velocities of (a, c) 1 μm/s and (b, d) 10 μm/s. (a, b) Manipulation on the end part of the NW. (c, d) Manipulation on the middle part. The inset AFM images were obtained after the manipulation on different positions.

In conclusion, the tip-driving velocity can lead to a difference in the lateral manipulation of NWs. Relatively low velocity and end position can be used for the movement of NWs with high precision, and hence are recommended for manipulation. Based on the results in Figure 4, it can be deduced that the initial interfacial interactions

between the NW and the substrate contribute greatly to the sudden increase in lateral force during manipulation. The adhesion between the NW and the substrate contributes chiefly to the lateral force at the beginning of the NW moving from its original place. As shown in Figure 4, the adhesion force may correspond with the lateral force of 150-550 nN, which is much higher than the gravity of a 15 μm-long Ag NW, 1.85×10^{-5} nN.

Cross-section microstructures. For further investigating the mechanical deformations during bending, indentation, and lateral manipulation, the cross-section microstructure of individual Ag NW was prepared for high-resolution TEM detection. Figure 5a showed a separated NW on Si (100) substrate selected for subsequent observation. Before focused ion beam (FIB) cutting, protective layers of polymer and Pt were deposited in turn to prevent the NW and the Si surface from being destroyed.[34,35] From Figure 5b, grain boundaries were detected inside Ag NWs, which may cause relative displacement between the grains in each region when a load was applied from the outside. It was hence expected that the presence of grain boundaries can cause the crack generation[36] in Ag NWs during the AFM indentation test or lateral bending. Furthermore, the thin interfacial film of ~3.7 nm between the NW and the substrate was analyzed, as displayed in Figure 5c. Energy dispersion spectrum (EDS) analysis was performed on the interface of the Ag NW/substrate to identify chemical compositions. As can be seen in Figure 5d, elements of C, O, Si and Ag were detected from the interface. Although quantitative analysis was difficult, it can still be judged that the interface was dominated by carbon compounds, silver oxide, silicon oxide, and their interaction. The interfacial film may contribute greatly to the adhesion[37,38] during

the manipulation by an AFM probe, which plays a key role in the mechanical manipulation of NWs.[21] For one thing, weak interaction between the NW and the substrate can promote the manipulation. For another, necessary interfacial interaction can ensure the stabilization of the assembled NWs. Therefore, controlling the interface is challenging but significant for manipulating NWs.

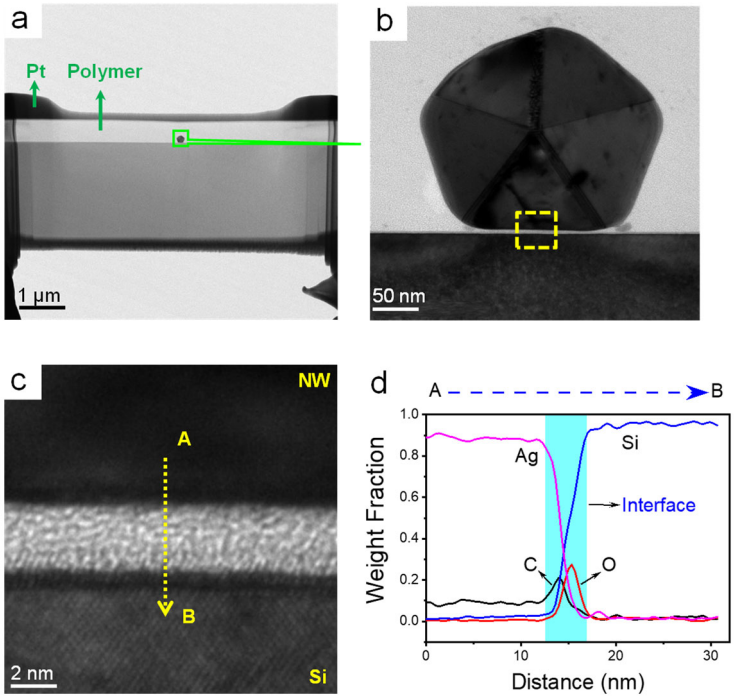

Figure 5. High-resolution TEM detection of the cross-section of the Ag NW. (a) X-cut of the Ag NW on Si surface by FIB milling. (b) Cross section of the Ag NW. (c) High-resolution TEM image of the NW/Si interface. (d) The weight fractions of C, O, Ag, and Si plotted as the distance along A to B as marked on (c) by EDS analysis.

In summary, controlling the interfacial interactions between the NW and the substrate is of significance for lateral or two-dimensional manipulation through an engineered trajectory. The high adhesion between NW and the substrate should be

reduced for the ease of movement, and a low-adhesive substrate surface is also required. After the manipulation, the fixing of NWs on a new host substrate becomes important for the stability of NWs-based devices. Moreover, for fabricating high-performance devices, three-dimensional manipulation of NWs is vital for spatial assembling, offering great potential as building blocks for applications in nanoelectronics and photonics.[5,10,11]

CONCLUSION

In conclusion, the lateral bending of Ag NWs was investigated under different tip-driven velocities and manipulation positions. Firstly, the bending-deformation of individual Ag NW was detected by AFM scanning and *in-situ* SEM observation, respectively, for obtaining more details of the bent part. It was found that the fracture occurred in the bending part when the bending angle was larger than 80°. Compared to Ag substrate, Ag NWs presented a lower system stiffness by the nanoindentation with AFM. High-resolution TEM observations indicated that there existed grain boundaries inside Ag NWs, which may be the contributor to the fracture and the crack of Ag NWs during bending and nanoindentation. Based on the obtained mechanical property data, a series of tests were performed to seek the optimal manipulation position and velocity.

EXPERIMENTAL SECTION

Ag NWs from XFNANO Materials Tech Co, Ltd (Nanjing, China) prepared by solvothermal reduction were employed in the present tests. The diameter and length of NWs were ~200 nm and 10-20 μm, respectively. The NWs were dispersed on Si substrates by absolute ethanol for the manipulation with AFM (MFP-3D Infinity,

Oxford Instruments, UK). Nanoindentation and manipulation tests were performed using an AFM probe (NCHV, Bruker, USA) with a normal spring constant of 42 nN/nm. AFM contact mode was used for lateral bending and manipulation of Ag NWs, and *in-situ* topographies of the NWs were obtained by the AFM under tapping mode and by SEM (Gemini 300, ZEISS, Germany), respectively. The manipulation of NWs was conducted in air at a relative humidity of ~55% and a temperature of ~25 °C. For investigating mechanical properties, High-resolution TEM (Tecnai G2 F20, FEI, USA) detection was carried out on the cross-section of the Ag NW. Before TEM observations, a protective polymer layer followed by a Pt coating was deposited on the sample, and then FIB (Nanolab Helios 400S, FEI, USA) cutting was utilized to obtain the cross-section structure of the Ag NW.

AUTHOR INFORMATION

Corresponding Authors

Huiyun Liu − *Department of Electronic & Electrical Engineering, University College London, London WC1E 7JE, U.K;* E-mail: huiyun.liu@ucl.ac.uk

Linmao Qian − *Tribology Research Institute, School of Mechanical Engineering, Southwest Jiaotong University, Chengdu 610031,* China; E-mail: linmao@swjtu.edu.cn

Bingjun Yu − *Tribology Research Institute, School of Mechanical Engineering, Southwest Jiaotong University, Chengdu 610031, China;* E-mail: bingjun@swjtu.edu.cn

Authors

Licong Cui − *Tribology Research Institute, School of Mechanical Engineering, Southwest Jiaotong University, Chengdu 610031, China*

Jiaming Li − *ZTE Corporation, Chengdu 610299, China*

Huaicheng Zhou − *Tribology Research Institute, School of Mechanical Engineering, Southwest Jiaotong University, Chengdu 610031, China*

Lei Wu − *Tribology Research Institute, School of Mechanical Engineering, Southwest Jiaotong University, Chengdu 610031, China*

Dan Yang − *Tribology Research Institute, School of Mechanical Engineering, Southwest Jiaotong University, Chengdu 610031, China*

Notes

The authors declare no competing financial interest.

ACKNOWLEDGMENTS

The authors would like express thanks to the National Natural Science Foundation of China (52175549), and the Fundamental Research Funds for the Central Universities (2682021ZTPY055).

REFERENCES

(1) Fu, B.; Sun, J.-X.; Cheng, Y.; Ouyang, H.; Compagnini, G.; Yin, P.; Wei, S.-R.; Li, S.-J.; Li, D.-B.; Scardaci, V.; Zhang, H. Recent Progress on Metal-Based Nanomaterials: Fabrications, Optical Properties, and Applications in Ultrafast Photonics. *Adv. Funct. Mater.* 2021, 31, 2107363.

(2) Li, H.-X.; Zhou, X.-C.; Zhai, W.; Lu, S.-Y.; Liang, J.-Z.; He, Z.; Long, H.-W.; Xiong, T.-T.; Sun, H.-Y.; He, Q.-Y.; Fan, Z.-X.; Zhang, H. Phase Engineering of

Nanomaterials for Clean Energy and Catalytic Applications. *Adv. Energy Mater.* 2020, 40, 2002019.

(3) Park, W.; Shin, H.; Choi, B.; Rhim, W.; Na, K.; Han, D.-K. Advanced Hybrid Nanomaterials for Biomedical Applications. *Prog. Mater. Sci.* 2020, 114, 10068.

(4) Qiu, X.-Y.; Zhang, Y.; Zhu, Y.-F.; Long, C.; Su, L.-N.; Liu, S.-Q.; Tang, Z.-Y. Applications of Nanomaterials in Asymmetric Photocatalysis: Recent Progress, Challenges, and Opportunities. *Adv. Mater.* 2021, 33, 2001731.

(5) Wong-Leung, J.; Yang, I.; Li, Z.-Y.; Karuturi, S. K.; Fu, L.; Tan H.-H.; Jagadish, C. Engineering III–V Semiconductor Nanowires for Device Applications. *Adv. Mater.* 2020, 32, 1904359.

(6) Nehra, M.; Dilbaghi, N.; Marrazza, G.; Kaushik, A.; Abolhassani, R.; Mishra, Y. K.; Kim, K. H.; Kumar, S. 1D Semiconductor Nanowires for Energy Conversion, Harvesting and Storage Applications. *Nano Energy* 2020, 76, 104991.

(7) Zhang, R.-G.; Liang, P.; Yang, H.; Min, H.-H.; Niu, M.-M.; Jin, S.-Y.; Jiang, Y.-T.; Pan, Z.-G.; Yan, J.-X.; Shen, X.-D.; Wang, Jin. Manipulating Intercalation-Extraction Mechanisms in Structurally Modulated δ-MnO_2 Nanowires for High-Performance Aqueous Zinc-Ion Batteries. *Chem. Eng. J.* 2022, 433, 133687.

(8) Xu, C.-T.; Zou, R.-J.; Peng, Y.-X.; Liu, Q.; Ruan S.-C.; Hu, J.-Q. In Situ Transmission Electron Microscope Studies on One-Dimensional Nanomaterials: Manipulation, Properties and Applications. *Prog. Mater. Sci.* 2020, 113, 10067.

(9) Dai, T.-T.; Deng, Z.-H.; Fang, X.-D.; Lu, H.-D.; He, Y.; Chang, J.-Q.; Wang, S.-M.; Zhu, N.-W.; Li, L.; Meng, G. In Situ Assembly of Ordered Hierarchical CuO Microhemisphere Nanowire Arrays for High-Performance Bifunctional Sensing Applications. *Small Methods* 2021, 6, 2100202.

(10) Wang, J.-L.; Liu, J.-W.; Sheng, S.-Z.; He, Z.; Gao, J.; Yu, S.-H. Manipulating Nanowire Assemblies Toward Multicolor Transparent Electrochromic Device. *Nano Lett.* 2021, 21, 9203-9209.

(11) Takiguchi, M.; Takemura, N.; Tateno, K.; Nozaki, K.; Sasaki, S.; Sergent, S.; Kuramochi, E.; Wasawo, T.; Yokoo, A.; Shinya, A.; Notomi, M. All-Optical InAsP/InP Nanowire Switches Integrated in a Si Photonic Crystal. *ACS Photonics* 2020, 7, 1016−1021.

(12) Zheng, D.-S.; Wang, H.-L.; Chen, R.-L.; Li, L.; Guo, J.-X.; Gu, Y.; Zubair, M. M.; Yu, X.-X.; Jiang, L.; Zhu, D.-S.; Xiong, Y.; Zhang, H.; Yang W.-X.; Miao, J.-S. High-Detectivity Tin Disulfide Nanowire Photodetectors with Manipulation of Localized Ferroelectric Polarization Field. *Nanophotonics* 2021, 10, 4637-4644.

(13) Taaber, T.; Antsov, M.; Vlassov, S.; Mäeorg, U.; Dorogin, L.; Järvekülg, M.; Saal, K.; Lõhmus, R. Formation and Characterization of Microcantilevers Produced from Ionic Liquid by Electron Beam Irradiation. *J. Mol. Liq.* 2017, 229, 45-50.

(14) Moreno-Moreno, M.; Ares, P.; Moreno, C.; Zamora, F.; Gómez-Navarro, C.; Gómez-Herrero, J. AFM Manipulation of Gold Nanowires to Build Electrical Circuits. *Nano Lett.* 2019, 19, 5459-5468.

(15) Zhang, T.-Y.; Yu, H.-B.; Li, P.; Wang, X.-D.; Wang, F.-F.; Shi, J.-L.; Liu, Z.; Yu, P.; Yang, W.-G.; Wang, Y.-C.; Liu, L.-Q. Microsphere-Based Super-Resolution Imaging for Visualized Nanomanipulation. *ACS Appl. Mater. Inter.* 2020, 12, 48093-48100.

(16) Bai, H.-T.; Wu, S. Deep-Learning-Based Nanowire Detection in AFM Images for Automated Nanomanipulation. *Nanotechnol. Precis. Eng.* 2021, 4, 013002.

(17) Ye, X.-T.; Zhang, Y.; Ru, C.-H.; Luo, J.; Xie, S.-R.; Sun, Y. Automated Pick-Place of Silicon Nanowires. *IEEE T. Autom. Sci. Eng.* 2013, 10, 554-561.

(18) Liu, H.-Z.; Wu, S.; Zhang, J.-M.; Bai, H.-Y.; Jin, F.; Pang, H.; Hu, X.-D. Strategies for the AFM-Based Manipulation of Silver Nanowires on a Flat Surface. *Nanotechnology* 2017, 28, 365301.

(19) Bartenwerfer M.; Fatikow, S. Directed Nanorobot-Based Handling of Single Nanowires. 2011 IEEE International Conference on Mechatronics and Automation, Beijing, China, 07-10 August; IEEE, 2011; 183-188.

(20) Toku, Y.; Kobayashi, K.; Muraoka, M. Repositioning Technique in Nanowire Manipulation by Oscillating Gripper. *Micro. Nano. Lett.* 2013, 8, 63-65.

(21) Xie, H.; Haliyo, D. S.; Régnier, S. A Versatile Atomic Force Microscope for Three-Dimensional Nanomanipulation and Nanoassembly. *Nanotechnology* 2009, 20, 215301.

(22) Xie, H.; Régnier, S. In Situ Peeling of One-Dimensional Nanostructures Using a

Dual-Probe Nanotweezer. *Rev. Sci. Instrum.* 2010, 81, 035112.

(23) Noel, O.; Mazeran, P. E.; Nasralla, H. Sliding Velocity Dependence of Adhesion in a Nanometer-Sized Contact. *Phys. Rev. Lett.* 2012, 108, 015503.

(24) Hou, L.-Z.; Mead, J.-L.; Wang, S.-L.; Huang, H. The Kinetic Frictional Shear Stress of ZnO Nanowires on Graphite and Mica Substrates. *Appl. Surf. Sci.* 2019, 465, 584-590.

(25) Stan, G.; Krylyuk, S.; Davydov, A. V.; Levin, I.; Cook, R. F. Ultimate Bending Strength of Si Nanowires. *Nano Lett.* 2012, 12(5), 2599-2604.

(26) Zeng, X.-Z.; Peng, Y.-T.; Lang, H.-J.; Cao, X.-A. Nanotribological Behavior of a Single Silver Nanowire on Graphite. *Nanotechnology* 2018, 29, 085706.

(27) Park, H. S.; Cai, W.; Espinosa, H. D.; Huang, H.-C. Mechanics of Crystalline Nanowires. *MRS Bull.* 2009, 34, 178-183.

(28) Adams, G. G.; Nagappan, P.; McGruer, N. E. Continuum Modeling and Analysis of the Frictional Interaction Between a CNT and a Substrate During Dragging. *J. Tribol-T ASME* 2009, 13, 163-170.

(29) Moradi, M.; Fereidon, A. H.; Sadeghzadeh, S. Aspect Ratio and Dimension Effects on Nanorod Manipulation by Atomic Force Microscope. *Micro. Nano. Lett.* 2010, 5, 324-327.

(30) Tran, D. K.; Chung, K. H. Simultaneous Measurement of Elastic Properties and Friction Characteristics of Nanowires Using Atomic Force Microscopy. *Exp. Mech.*

2015, 55, 903-915.

(31) Kim, H. J.; Nguyen, G. H.; Cao Ky, D. L.; Tran, D. K.; Jeon, K. J.; Chung, K. H. Static and Kinetic Friction Characteristics of Nanowire on Different Substrates. *Appl. Surf. Sci.* 2016, 379, 452-461.

(32) Marshall, S. J.; Bayne, S. C.; Baier, R.; Tomsia, A. P.; Marshall, G. W. A Review of Adhesion Science. *Dent. Mater.* 2010, 26, 11-16.

(33) Colak, A.; Wormeester, H.; Zandvliet, H. J. W.; Poelsema, B. The Influence of Instrumental Parameters on the Adhesion Force in a Flat-on-Rough Contact Geometry. *Appl. Surf. Sci.* 2015, 353, 1285-1290.

(34) Wu, L.; Cui, L.-C.; He, W.; Guo, J.; Yu, B.-J.; Qian, L.-M. Toward Controllable Wet Etching of Monocrystalline Silicon: Roles of Mechanically Driven Defects. *ACS Appl. Mater. Inter.* 2022, 14, 29366-29376.

(35) Wu, L.; Shang, K.-D.; Chen, T.-T.; Feng, C.-Q.; Yang, T.-T.; Zhao, Z.-J.; Yu, B.-J.; Qian L.-M. Template-Free Lithography for Cross-Scale Channels Towards Enhancing Nanofluidic Devices. *Sensor. Actuat. B-Chem* 2022, 372, 132642.

(36) Liu, C.-Y.; Zhang, Y.-S.; Kao, C.-K.; Liu, J.-H. Fabrication of Silver Nanowires Via a β-Cyclodextrin-Derived Soft Template. *Express Polym. Lett.* 2018, 12, 591-599.

(37) Deng, B.; Hsu, P.-C.; Chen, G.-C.; Chandrashekar, B. N.; Liao, L.; Ayitimuda, Z.; Wu, J.-X.; Guo, Y.-F.; Lin, L.; Zhou, Y.; Aisijiang, M.; Xie, Q.; Cui, Y.; Liu, Z.-F.;

Peng, H.-L. Roll-to-Roll Encapsulation of Metal Nanowires Between Graphene and Plastic Substrate for High-Performance Flexible Transparent Electrodes. *Nano Lett.* 2015, 15, 4206-4213.

(38) Lee, J.; Lee, P.; Lee, H. B.; Hong, S.; Lee, I.; Yeo, J.; Lee, S. S.; Kim, T. S.; Lee, D. J.; Ko, S. H. Room-Temperature Nanosoldering of a Very Long Metal Nanowire Network by Conducting-Polymer-Assisted Joining for a Flexible Touch-Panel Application. *Adv. Funct. Mater.* 2013, 23, 4171-4176.

For Table of Contents Only